alyzed by a phosphoimager (Molecular Dynamics, Sunnydale, CA) as described (*6*). To visualize asters, we placed extract in an FC-47 chamber [G. Sluder *et al.*, *Meth. Cell Biol.* **61**, 439 (1998)] and viewed it with a modified Zeiss ACM microscope (Zeiss) with polarization optics and a charge-coupled device camera (Hammamatsu, East Bridgewater, NJ, or Dage-MTI, Michigan City, IL) at 20°C. Time-lapse video images were written directly to the hard drive of a PC, as described (*6*). Video sequence playback of aster doubling was done with Adobe Premiere Software (Mountain View, CA).

18. S. Ikegami, S. Amemiya, M. Ouro, H. Nagano, Y. Mano, *Nature* **275**, 458 (1978).
19. M. Lohka and J. L. Maller, *J. Cell Biol.* **101**, 518 (1985); J. J. Blow and R. A. Laskey, *Cell* **47**, 577 (1986).
20. E. H. Hinchcliffe, C. Li, E. A. Thompson, J. L. Maller, G. Sluder, data not shown.
21. M. Dasso and J. W. Newport, *Cell* **61**, 811 (1990).
22. F. Tournier, M. Cyrklaff, E. Karsenti, M. Bornens, *Proc. Natl. Acad. Sci. U.S.A.* **88**, 9929 (1991); R. Heald *et al.*, *Nature* **382**, 420 (1996).
23. G. Sluder and C. L. Rieder, *J. Cell Biol.* **100**, 887 (1985).
24. J. Y. Su, R. E. Rempel, E. Erickson, J. L. Maller, *Proc. Natl. Acad. Sci. U.S.A.* **92**, 10187 (1995).
25. J. W. Harper and S. J. Elldrege, *Curr. Opin. Gen. Dev.* **6**, 56 (1996).
26. U. P. Strausfeld *et al.*, *J. Cell Sci.* **109**, 1555 (1996).
27. Glutathione S-transferase–tagged fusion proteins of Δ34Xic1 and C-Xic1 were prepared and purified as described (*13*, *24*). Recombinant *Xenopus* Cdk2-E complex was expressed, purified, and tested for kinase activity in vitro as described (*13*, *24*).
28. Immunofluorescence staining of *Xenopus* embryos was done as described (*8*), with affinity-purified polyclonal antibody to cyclin E (*9*) and monoclonal antibodies to α tubulin or γ tubulin (Sigma). Confocal microscopy was performed on an MRC-600 system (Bio-Rad, Hercules, CA). The confocal images presented represent projections of Z-series scans.
29. E. Bailly, J. Pines, T. Hunter, M. Bornens, *J. Cell Sci.* **101**, 529 (1992).
30. We thank F. J. Miller for help developing the observation chambers, C. Wilkerson and M. Cham for assistance in building the image acquisition computers, and R. Pope, T. Pederson, G. Witman, and B. Luna for comments on the manuscript. Supported by the NIH (J.L.M. and G.S.), the Trustees of the Worcester Foundation (G.S.), and the Cabot Family Charitable Trust (G.S.). J.L.M. is an investigator of the Howard Hughes Medical Institute. E.H.H. is supported by an NIH postdoctoral training fellowship. The authors would like to dedicate this work to the memory of Dan Mazia.

6 October 1998; accepted 12 January 1999

Mycolactone: A Polyketide Toxin from *Mycobacterium ulcerans* Required for Virulence

Kathleen M. George,[1] Delphi Chatterjee,[2] Geewananda Gunawardana,[3] Diane Welty,[1] John Hayman,[4] Richard Lee,[5] P. L. C. Small[1]*

Mycobacterium ulcerans is the causative agent of Buruli ulcer, a severe human skin disease that occurs primarily in Africa and Australia. Infection with *M. ulcerans* results in persistent severe necrosis without an acute inflammatory response. The presence of histopathological changes distant from the site of infection suggested that pathogenesis might be toxin mediated. A polyketide-derived macrolide designated mycolactone was isolated that causes cytopathicity and cell cycle arrest in cultured L929 murine fibroblasts. Intradermal inoculation of purified toxin into guinea pigs produced a lesion similar to that of Buruli ulcer in humans. This toxin may represent one of a family of virulence factors associated with pathology in mycobacterial diseases such as leprosy and tuberculosis.

Most pathogenic bacteria produce toxins that are important in disease. However, none has been identified for *Mycobacterium tuberculosis* and *Mycobacterium leprae*. The only mycobacterial pathogen for which there is any evidence of toxin production is *Mycobacteria ulcerans*, the causative agent of Buruli ulcer. Although Buruli ulcer is little known outside the tropics, it recently has been recognized as an emerging infection in western Africa (*1*). *Mycobacterium ulcerans* disease has several distinctive features. Infection results in progressive necrotic cutaneous lesions, which may persist for a decade if untreated and may extend to 15% of a patient's skin surface. Despite extensive necrosis, lesions are painless, symptoms of systemic disease are absent, and there is little histological evidence of an initial acute inflammatory response (*2*, *3*). Finally, in contrast to other pathogenic mycobacteria, which are facultative intracellular parasites of macrophages, *M. ulcerans* occurs in lesions primarily as extracellular microcolonies.

A curious feature of Buruli ulcer pathology is that organisms lie in a necrotic focus with the necrosis extending some distance from the site of bacterial colonization. This observation led to the hypothesis that *M. ulcerans* secreted a toxin (*2*). In 1974, Read *et al.* reported that a sterile filtrate of *M. ulcerans* had a cytopathic effect on cultured murine fibroblasts (*4*). Early efforts to isolate this toxin were not successful (*5*, *6*). More recently, Pimsler *et al.* (*7*) reported that a sterile filtrate of *M. ulcerans* had immunosuppressive properties. Earlier this year, we reported cytotoxic activity associated with acetone-soluble lipids (ASL) present in an organic extract from *M. ulcerans* sterile filtrate (*8*). The cytopathic effect of *M. ulcerans* or ASL on L929 murine fibroblasts was further characterized by showing that *M. ulcerans* or ASL arrested cells in the G_0/G_1 stage of the cell cycle. In this paper, we report the purification of this toxin and present evidence for its role in the pathogenesis of Buruli ulcer.

Initial attempts to obtain sufficient toxin from *M. ulcerans* sterile filtrate for structural analysis were frustrated by low yield. To increase yield, we developed a method for isolating toxin from intact bacteria (*9*). ASL were prepared from an extract of *M. ulcerans* containing chloroform and methanol (2:1) and were separated by thin-layer chromatography (TLC) on silica gel plates. Lipid bands were eluted from TLC plates and tested for cytopathicity on L929 mouse fibroblast cells as described (*8*). Maximum toxic activity was associated with a light yellow, ultraviolet-active component (*10*) with a refractive index of 0.23 in a solvent system containing chloroform, methanol, and water (90:10:1) (Fig. 1A). This compound was further purified by reversed-phase high-performance liquid chromatography and subjected to structural analysis. Mass spectral analysis of the toxin molecule under microspray conditions showed peaks at *m/z* 765 (strong), 743 (weak), and 725 (medium) (Fig. 1B). Accurate mass measurement of the peak at *m/z* 765 (M^+ + Na: $C_{44}H_{70}O_9Na$, observed 765.4912; calculated 765.4912; error <0.1 ppm) and the peak at *m/z* 725 (M^+-OH: $C_{44}H_{69}O_8$, observed 725.4988; calculated 725.4987; error = 0.1 ppm) gave the formula $C_{44}H_{70}O_9$ for the compound. The compound was identified by two-dimensional nuclear magnetic resonance spectral analysis as a polyketide-derived 12-membered ring macrolide (Fig. 2) (*11*). The toxin was named mycolactone to reflect its mycobacterial source and chemical structure.

To determine whether mycolactone was cytopathic, we applied serial dilutions of sterile filtrate or mycolactone to an overnight culture of L929 cells. Within 24 hours after addition of mycolactone, the cells rounded up and by 48 hours most cells lifted off the plate (Fig. 1C).

[1]Rocky Mountain Laboratories, National Institute of Allergy and Infectious Diseases, National Institutes of Health, Hamilton, MT 59840, USA. [2]Department of Microbiology, Colorado State University, Fort Collins, CO 80523-1677, USA. [3]Abbott Laboratories, Abbott Park, IL 60064, USA. [4]Box Hill Hospital, Box Hill, Victoria 3128 Australia. [5]National Institute of Allergy and Infectious Diseases, National Institutes of Health, Rockville, MD 20852, USA.

*To whom correspondence should be addressed. E-mail: psmall@nih.gov

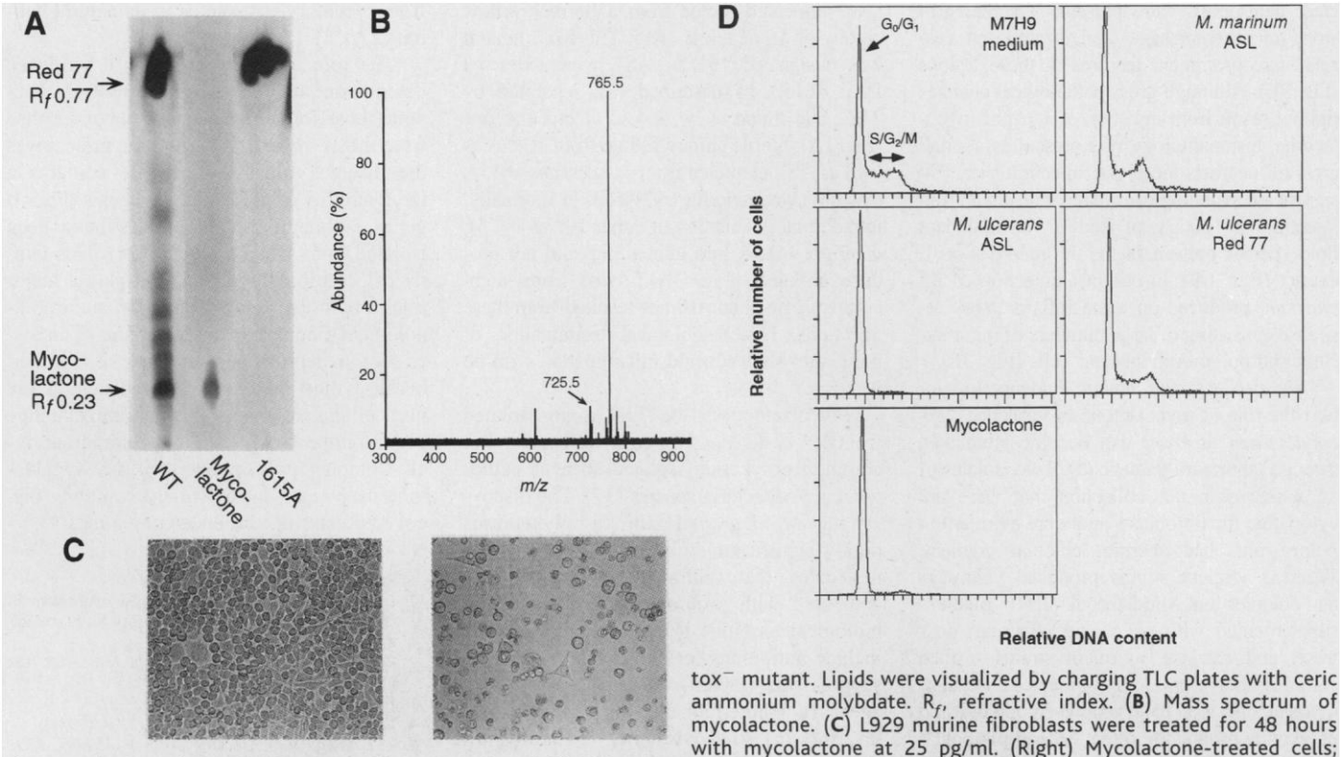

Fig. 1. Isolation of mycolactone and effects on cultured fibroblasts. (**A**) Mycolactone as a major lipid species in ASL from *M. ulcerans*, run on silica TLC, and with chloroform, methanol, and water (90:10:1) used as a solvent system. Several mycolactone-derived degradation products appear between R_f 0.3 and 0.6. Lane WT, wild type; lane mycolactone, purified mycolactone; lane 1615A, ASL from isogenic tox$^-$ mutant. Lipids were visualized by charging TLC plates with ceric ammonium molybdate. R_f, refractive index. (**B**) Mass spectrum of mycolactone. (**C**) L929 murine fibroblasts were treated for 48 hours with mycolactone at 25 pg/ml. (Right) Mycolactone-treated cells; (left) control monolayer. ×100. (**D**) Flow cytometric analysis of L929 cells treated with ASL or mycolactone from *M. ulcerans* (*13*). Cells exposed to *M. ulcerans* ASL (1 μg/ml), mycolactone (1 μg/ml), or control lipids (1 μg/ml) were lysed after 48 hours in the presence of RNase, stained with propidium iodide, and analyzed with FACStar for a cell cycle profile.

Washed cells were capable of regrowth, which indicated that the effect of toxin was reversible. Mycolactone at a concentration of 25 pg/ml was sufficient for cytopathicity. Chemical modification of mycolactone by acetylation of hydroxyl groups or hydrogenation that resulted in saturation of double bonds led to ablation of cytopathic activity (*12*). We had previously shown that *M. ulcerans*–derived ASL-treated cells were arrested in G_0/G_1 of the cell cycle (*8*). Flow cytometric analysis of the mycolactone-treated cell population showed that treatment of L929 cells with mycolactone arrested cells in G_0/G_1 of the cell cycle (Fig. 1D). These studies confirmed that the morphological changes and kinetics of cytopathicity reported previously with *M. ulcerans* ASL or sterile filtrate could be entirely reproduced by mycolactone alone.

To determine whether mycolactone-mediated cytopathicity was a correlate of in vivo virulence, Mycolactone was tested in a guinea pig model of virulence (*14*). The extensive necrosis in the absence of an acute inflammatory response is well preserved in the guinea pig model of infection (*5*). For these studies, we injected samples intradermally into the shaved back of six Hartley guinea pigs, and examined animals daily for evidence of gross pathological changes (*15*). Two guinea pigs were killed 2, 8, and 20 days after injection, and tissue was excised for histopathological analysis. Within 24 hours after injection, erythema was present at the site of highest mycolactone concentration (100 μg). Gross pathology was absent from all other injection sites at that time. The area injected with 100 μg of mycolactone increased in size until day 5 when the lesion appeared as a dark, necrotic, open wound. The lesion remained essentially the same until day 8 when tissue was harvested (Fig. 3A). Pressure applied to the necrotic area did not elicit a response from the guinea pig, which suggests that the lesion was painless. We observed slight erythema near the injection site of 10 μg of mycolactone on day 3 but a lesion did not develop. Injection of 1 μg of mycolactone was negative for gross pathology. Injection of 10^7 *M. ulcerans* produced slight erythema by day 3; by day 8 a small, open lesion was present (Fig. 3A). Although the upper dermis sloughed off the top of lesions where both mycolactone and *M. ulcerans* had been injected, resulting in a depressed ulcer, a purulent exudate was never present. In contrast, injection of 10^7 *Mycobacterium marinum* resulted in a purulent pus-filled lesion by day 5. No gross pathological changes resulted from the injection of 100 μl of mycobacterial medium or 100 μg of Red 77, an abundant lipid species present in the ASL fraction from which mycolactone was purified.

Histopathological findings (Fig. 3) demonstrated that the cellular damage resulting from injection of mycolactone and *M. ulcerans* bacteria was nearly identical (Fig. 3, C and E). An examination of paraffin-embedded sections stained with hematoxylin and eosin revealed the characteristic pathology of Buruli ulcer. Focal necrosis extended through the dermis and adipose tissue and into muscle. Despite considerable tissue destruction, few polymorphonu-

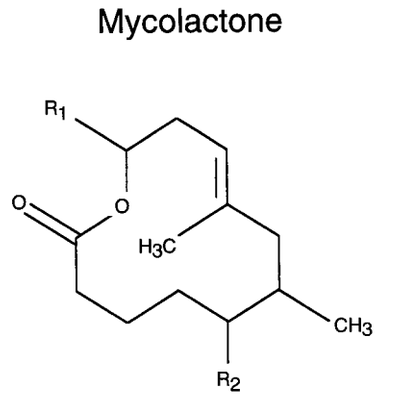

Fig. 2. Mycolactone is composed of a 12-membered ring to which two polyketide-derived side chains (R_1 and R_2) are attached.

clear neutrophils were present. Vascular erosion, microhemorrhage, and thrombosed vessels were prominent features in these lesions (Fig. 3E). Although gross pathological changes did not result from injection of 1 μg of mycolactone, histopathology was present as a small area of necrosis near the injection site. No significant pathological changes resulted from injection of 100 μg of Red 77, an abundant lipid species present in the *M. ulcerans* ASL extract (Fig. 1A). In contrast, injection of *M. marinum* produced an acute inflammatory response consisting of large numbers of mononuclear and polymorphonuclear cells (Fig. 3F).

We also obtained genetic evidence to support the role of mycolactone in virulence. *Mycobacterium ulcerans* can become attenuated through laboratory passage (*5*). Two isolates of *M. ulcerans* in our collection that were not cytopathic for fibroblasts and were avirulent in guinea pigs had aberrant colonial pigment. Whereas virulent strains produced yellowish tan colonies on Middlebrook 7H10 medium supplemented with oleic acid, albumin, dextrose, and catalase, avirulent strains formed colonies that were less pigmented. Because mycolactone is a pale yellow compound and polyketide production often leads to pigmentation in *Streptomyces* species, we thought that the lack of pigment might be a marker for toxin loss. Examining aged cultures, we isolated an isogenic mutant of *M. ulcerans* by selecting a less pigmented sector from a normal yellow colony of *M. ulcerans* 1615. This tox$^-$ mutant was designated 1615A. ASL were extracted from 1615A as described (*8*), separated by TLC, and found to be devoid of mycolactone (Fig. 1A). Sterile culture filtrate from 1615A as well as ASL extracted from *M. ulcerans* 1615A was not cytopathic for L929 cells (*16*). Finally, intradermal inoculation of either 10^8 or 10^7 *M. ulcerans* 1615A into guinea pigs did not produce an ulcer (Fig. 3A). Aside from slight erythema, no abnormalities resulted from these injections. Histopathological examination of these sites showed mild inflammation with no necrosis.

Mycolactone is the first toxin isolated from *Mycobacteria* species as well as the first complex polyketide isolated from a pathogenic mycobacteria species (*17*). The discovery that *M. ulcerans* toxin is a polyketide is highly significant. Polyketides are lipid-like molecules that, although relatively small compared with protein toxins, have potent biological activities. Well-known polyketides include antibiotics (erythromycin), immunosuppressants, (rapamycin, FK506), antifungal agents (amphotericin B), antihelmetic agents (avermectin), and cytostatins (bafilomycin). Most complex polyketides are made as secondary metabolites by soil bacteria in the order Actinomycetales (*18–21*). We speculate that mycolactone protects *M. ulcerans* from predatory eukaryotes in its natural habitat (*22, 23*).

The role of mycolactone as a virulence determinant may have implications far beyond those for Buruli ulcer. A major surprise from the *M. tuberculosis* genome project was the discovery that the genome contains a large number of polyketide synthesis (PKS I) genes, although no polyketides have been isolated from *M. tuberculosis* (*24*). This family of potent compounds could play a major role in both the tissue destruction and immunological modulation characteristic of diseases such as leprosy and tuberculosis. Further, because most pathogenic mycobacteria are intracellular pathogens, it is possible that they play an important role in intracellular survival. Complex polyketides such as Mycolactone may represent the first of a newly discovered class of virulence compounds.

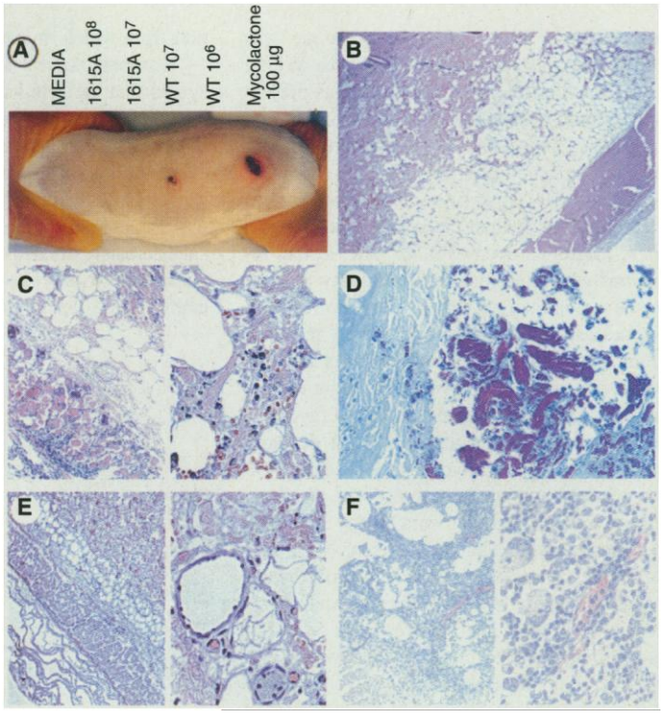

Fig. 3. Pathology in guinea pig skin after intradermal injection of mycolactone and *M. ulcerans* 8 days after infection. (**A**) Injection of mycobacterial medium or tox$^-$ mutant *M. ulcerans* 1615A did not produce a lesion, whereas injection of either viable *M. ulcerans* or 100 μg of mycolactone resulted in formation of a necrotic, noninflammatory lesion. Histopathology was evaluated from paraffin-embedded sections stained with hematoxylin and eosin. WT, wild type. (**B**) Injection of mycobacterial medium used as a control. (**C**) (left) Injection of *M ulcerans*. (Right) Microhemorrhage and necrosis throughout the fat layer extending into the muscle were frequent findings. (**D**) Zeihl-Neelson staining showing typical large clusters of predominantly extracellular *M. ulcerans*. (**E**) Injection of 10 μg of mycolactone. Occluded vessels (right) were frequently found in areas of necrosis. (**F**) Injection of *M. marinum*. (B) and (C) (left), (E) (left), and (F) (left), ×40; (D) and (C) (right), (E) (right), and (F) (right), ×400.

References and Notes

1. C. R. Horsburgh and A. M. Nelson, Eds., *Pathology of Emerging Infections* (American Society for Microbiology Press, Herndon, VA, 1997).
2. D. H. Connor and F. H. Lunn, *Arch. Pathol.* **81**, 183 (1966).
3. J. Hayman, *J. Clin. Pathol.* **46**, 5 (1993).
4. J. K. Read *et al.*, *Infect. Immun.* **9**, 1114 (1974).
5. R. E. Krieg, W. T. Hockmeyer, D. H. Connor, *Arch. Dermatol.* **110**, 783 (1974).
6. W. T. Hockmeyer, R. E. Kreig, M. Reich, R. D. Johnson, *Infect. Immun.* **21**, 124 (1978).
7. M. Pimsler, T. A. Sponsler, W. M. Meyers, *J. Infect. Dis.* **157**, 577 (1988).
8. K. M. George, L. Barker, D. Welty, P. L. C. Small, *Infect. Immun.* **66**, 587 (1998).
9. For toxin production, *M. ulcerans* 1615 (Trudeau Collection Strain, Lake Saranac, NY) were grown in Middlebrook 7H9 medium supplemented with 0.2% (v/v) glycerol and 10% oleic acid, albumin, dextrose, and catalase enrichment (Difco) and incubated at 32°C. We harvested cells at late exponential growth phase by passage through a 0.22-μm filter. Bacteria were scraped off the filter, weighed, and extracted by stirring with chloroform and methanol (2:1) for 4 hours. We removed the bacterial debris by centrifugation, and added 0.2 volume of water to the supernatant. The organic phase was removed and dried in a rotoevaporator, and the remaining lipids were resuspended in ice-cold acetone to precipitate phospholipids. The ASL fraction was run on silica TLC to separate individual lipid components by using chloroform, methanol, and water (90:10:1) as a solvent system. Lipid bands were scraped off, and lipids were eluted in the organic solvent in which they were run. These lipids were dried down, weighed, and resuspended in acetone at 4°C. Under these conditions, mycolactone did not lose biological activity for 6 weeks.
10. Data not shown.
11. Structural data submitted in a separate paper to the *Journal of American Chemical Society*.
12. Data not shown.
13. For flow cytometric analysis we grew L929 cells in six-well tissue culture plates. After 12 hours, we added sample lipids to the cells. After 48 hours, cells were harvested, washed with 0.1 phosphate-buffered saline, and suspended in fluorescence-activated cell sorting buffer containing phosphate-buffered saline, 0.1% Nonidet P-40, 20 μg of ribonuclease (RNase) A per milliliter, and propidium iodide at 50 μg per 10^6 cells per milliliter. Cells were sorted and analyzed on a FACStar instrument modified for five-parameter operation (Becton Dickinson Immunocytometry Systems, San Jose, CA).
14. We used Hartley female guinea pigs for virulence studies. We chose a bacterial inoculum size (10^6 to 10^8) that would produce a lesion within 2 weeks. A consistent inoculum dose was obtained by passing bacteria five

times through a 25-gauge needle. We confirmed inoculum size by viable colony counts and used sonication to prepare a homogenous inoculum of lipids for injection of 100, 10, and 1 μg of mycolactone and 100 and 10 μg of the control *M. ulcerans* lipid Red 77. Guinea pigs were prepared for injection by shaving the back and were observed daily for signs of pathology. We used duplicate guinea pigs for each time point. Results shown are from a typical experiment, which was repeated three times.

. Lesions were excised for histopathological examination and fixed for 24 hours in 3.7% formaldehyde. Tissues were embedded in paraffin, cut in 4-μm-thick sections, and stained with hematoxylin and eosin. We stained tissues that had been inoculated with *M. ulcerans* or *M. marinum* with Zeihl-Neelson stain.

16. Data not shown.
17. A. T. Hudson, I. M. Campbell, R. Bentley, *Biochemistry* **9**, 3988 (1970).
18. M. Labro, *Int. J. Antimicrob. Agents* **10**, 11 (1998).
19. D. A. Hopwood and D. H. Sherman, *Annu. Rev. Genet.* **24**, 37 (1990).
20. L. Katz and S. Donadio, *Annu. Rev. Microbiol.* **47**, 875 (1993).
21. R. A. Maplestone, M. J. Stone, D. H. Williams, *Gene* **115**, 151 (1992).
22. F. Portaels *et al.*, *J. Clin. Microbiol.* **35**, 1097 (1997).
23. B. C. Ross *et al.*, *Appl. Environ. Microbiol.* **63**, 4135 (1997).
24. S. Cole *et al.*, *Nature* **393**, 537 (1998).
25. We thank L. Barker, B. Caughey, T. Schwan, and L. Katz for critical reading of this report. We express particular appreciation to D. Brooks for assistance with flow cytometry, C. Favara for her skillful preparation of sections for histopathology, and P. Brennan for his insight and support. Animal experiments were conducted under guidelines of the Animal Care and Use Committee at Rocky Mountain Laboratories.

22 September 1998; accepted 5 January 1999

Control of Viremia in Simian Immunodeficiency Virus Infection by CD8$^+$ Lymphocytes

Jörn E. Schmitz,[1]* Marcelo J. Kuroda,[1] Sampa Santra,[1] Vito G. Sasseville,[2]† Meredith A. Simon,[2] Michelle A. Lifton,[1] Paul Racz,[3] Klara Tenner-Racz,[3] Margaret Dalesandro,[4]‡ Bernhard J. Scallon,[4] John Ghrayeb,[4] Meryl A. Forman,[5] David C. Montefiori,[6] E. Peter Rieber,[7] Norman L. Letvin,[1] Keith A. Reimann[1]*

Clinical evidence suggests that cellular immunity is involved in controlling human immunodeficiency virus–1 (HIV-1) replication. An animal model of acquired immune deficiency syndrome (AIDS), the simian immunodeficiency virus (SIV)–infected rhesus monkey, was used to show that virus replication is not controlled in monkeys depleted of CD8$^+$ lymphocytes during primary SIV infection. Eliminating CD8$^+$ lymphocytes from monkeys during chronic SIV infection resulted in a rapid and marked increase in viremia that was again suppressed coincident with the reappearance of SIV-specific CD8$^+$ T cells. These results confirm the importance of cell-mediated immunity in controlling HIV-1 infection and support the exploration of vaccination approaches for preventing infection that will elicit these immune responses.

Defining the immune mechanisms responsible for controlling HIV-1 replication during primary and chronic infection will be important for understanding the immunopathogenesis of AIDS. The delineation of these mechanisms will also be useful to establish the goals of HIV-1 vaccine approaches. A number of clinical and experimental observations have implicated virus-specific cytotoxic T lymphocytes (CTLs) in this process. CD8$^+$ lymphocytes from infected individuals have been shown to inhibit HIV-1 replication in vitro (*1*). Control of the intense burst of viral replication seen in primary HIV-1 infection coincides with the appearance of virus-specific CTLs (*2*). Finally, potent virus-specific CTL responses have been observed in infected individuals with low viral loads and persistent, nonprogressive infections (*3*). However, these observations provide only circumstantial evidence for the role of virus-specific cellular immune responses in controlling HIV-1 infections.

We directly assessed the role of cellular immunity in controlling HIV-1 infection by means of the SIV of macaques (SIVmac)/rhesus monkey model of AIDS (*4*). In previous attempts to abrogate cell-mediated immune responses in lentiviral infections, only incomplete, transient CD8$^+$ lymphocyte depletion was achieved, and the studies were done with nonpathogenic lentiviruses (*5*). We observed that intravenous administration of the CD8-specific mouse-human chimeric monoclonal antibody cM-T807 resulted in near total depletion of CD8-bearing lymphocytes from the blood and lymph nodes of normal monkeys, whereas the CD4$^+$ T cell subset remained unchanged (*6*). We therefore characterized the replication of SIVmac in monkeys depleted of CD8$^+$ lymphocytes by this antibody.

As in HIV-1 infection of humans, primary infection of rhesus monkeys with SIVmac is characterized by an intense burst of virus replication followed by an abrupt decline in viremia presumably due to the emergence of immune responses that suppress virus replication (*7*) or, potentially, to exhaustion of target cells (*8*). To determine the contribution of CD8$^+$ lymphocyte–mediated immune responses to this control of viremia, we treated rhesus monkeys with cM-T807 or a control monoclonal antibody during primary SIVmac infection (*9*). The cM-T807 treatment resulted in total depletion of CD8$^+$ T cells from the blood of monkeys (Fig. 1, B and C). Near total elimination of CD8$^+$ lymphocytes was also achieved in lymph nodes (Fig. 2, A and B), where immunophenotypic analysis of sequential biopsies confirmed a 90 to 100% decline in CD8$^+$ T cells (*10*). However, the duration of CD8$^+$ lymphocyte depletion varied considerably among monkeys. In three of the six cM-T807–treated monkeys, CD8$^+$ T cell depletion was evident for 17 to 21 days (Fig. 1B). In the other three monkeys, CD8$^+$ lymphocyte depletion was considerably more persistent. CD8$^+$ T cells were depleted in these monkeys for 28 to 60 days (Fig. 1C). The duration of antibody-mediated depletion is partially age-dependent, and the variability we observed was consistent with that seen in normal rhesus monkeys that received similar treatment (*6*, *11*). Nevertheless, we achieved ≥18 days of near total CD8$^+$ lymphocyte depletion in all six monkeys, and the duration of cell depletion from lymph nodes was equal to, or longer than, that observed in the blood. The other lymphocyte subsets showed only the transient decline that is generally seen during the peak of SIVmac viremia irrespective of any antibody treatment (*7*).

To determine the effect of CD8$^+$ lymphocyte depletion on the control of SIVmac infection, we assessed virus replication by measuring plasma viral RNA and SIVmac Gag p27 antigen levels. In all six control mon-

[1]Division of Viral Pathogenesis, Beth Israel Deaconess Medical Center, Harvard Medical School, Boston, MA 02215, USA. [2]New England Regional Primate Research Center, Harvard Medical School, Southborough, MA 01772, USA. [3]Bernhard-Nocht-Institute for Tropical Medicine, 20359 Hamburg, Germany. [4]Centocor, Malvern, PA 19355, USA. [5]Beckman Coulter, Miami, FL 33196, USA. [6]Department of Surgery, Duke University Medical Center, Durham, NC 27710, USA. [7]Institute of Immunology, Technical University of Dresden, 01101 Dresden, Germany.

*To whom correspondence should be addressed. E-mail: jschmitz@caregroup.harvard.edu; kreimann@caregroup.harvard.edu

†Present address: Bristol-Myers Squibb, PRI, Department of Experimental Pathology, Princeton, NJ 08540, USA.

‡Present address: Cambridge Pharma Consultancy, North America Office, New York, NY 10022.